

[(Cu-Radical)₂-Ln]: Structure and Magnetic Properties of a Hetero-tri-spin Chain of Rings (Ln = Y^{III}, Gd^{III}, Tb^{III}, Dy^{III})

Xiufeng Wang,[†] Peng Hu,[†] Licun Li,^{*,†} and Jean-Pascal Sutter^{*,‡,§}

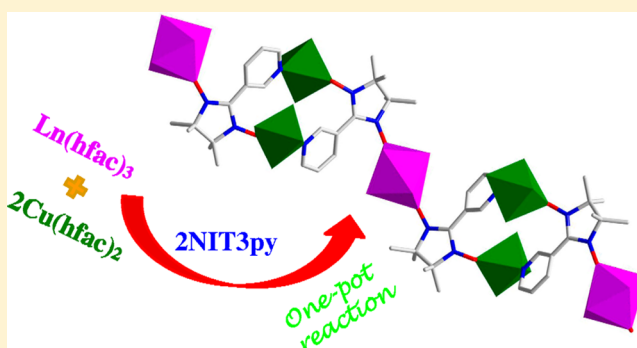
[†]Department of Chemistry, Key Laboratory of Advanced Energy Materials Chemistry and Tianjin Key Laboratory of Metal and Molecule-based Material Chemistry, Nankai University, Tianjin 300071, China

[‡]CNRS, LCC (Laboratoire de Chimie de Coordination), 205 Route de Narbonne, F-31077 Toulouse, France

[§]Université de Toulouse, UPS, INPT, LCC, F-31077 Toulouse, France

S Supporting Information

ABSTRACT: Novel hetero-tri-spin coordination polymers formed of ring-shaped Cu-nitronyl nitroxide spin clusters and Ln^{III} linkers are reported. These mixed 2p-3d-4f compounds of formula {[Ln(hfac)₃][Cu(hfac)₂(NIT-3Py)]₂·C₆H₁₄}_n [Ln^{III} = Y (1), Gd (2), Tb (3), and Dy (4); NIT-3Py = 2-(3-pyridyl)-4,4,5,5-tetramethylimidazoline-1-oxyl-3-oxide; hfac = hexa-fluoroacetylacetonate], exhibit a 1D chain structure consisting of [Cu(NIT-3Py)]₂ rings linked by Ln(hfac)₃ units. Their magnetic behavior is characteristic for ferromagnetic interactions between the metal centers and the coordinated radical units. The Tb derivative was found to exhibit slow relaxation of its magnetization.



INTRODUCTION

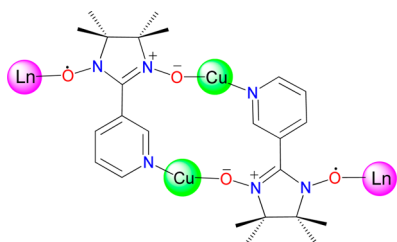
One-dimensional spin systems traditionally attract special interest in the domain of molecular magnetism, both from the physical and chemical points of view. Besides being excellent candidates for testing magnetic models which cannot be solved for high dimension systems,¹ 1D systems are associated with peculiar magnetic phenomena such as spin-Peierls transition² or haldane gap, among others.³ In recent years, slow magnetic relaxation, which is characteristic of Ising type 1D compounds,⁴ has attracted considerable attention.^{5,6} In the various chemical approaches to design one-dimensional compounds, one effective strategy involves nitronyl nitroxide radicals (NITR) as ligands.⁷ This radical with its two equivalent NO groups can act as a bridging ligand for two metal ions, thus allowing development of one-dimensional chain structures. Interestingly, the resulting exchange interaction between the spin carriers is the strongest possible as the result of the direct bonding of the moieties carrying the unpaired electrons.⁸ The first single chain magnet (SCM), [Co(hfac)₂(NIT-PhOMe)] has been achieved employing this approach.^{5a} Following this seminal example, several other NITR-cobalt as well as NITR-lanthanide chains exhibiting slow relaxation of their magnetization have been described recently.^{9,10} These compounds are characterized by a spin topology in which the radicals and the metal ions alternate, hence leading to chains with long-range correlation for the Ising spins. A related chemical approach is used for the construction of chains of SMMs, i.e. 1D organizations with no long-range ordering of the anisotropic spins. A modulation of the magnetic behavior for such systems is mainly achieved by varying the nature of the metal ion

(especially for the Ln based compounds)¹¹ and by chemical alteration at the periphery of the radical core to reduce the intermolecular interactions.¹² An alternative and appealing possibility to adjust the magnetic behaviors is to play with the spin topologies. Such an opportunity is offered by the systems with three different type spin carriers, i.e. hetero-tri-spin 2p-3d-4f compounds.¹³ Following the strategy using [3d-NIT] complexes as metallo-ligands we have introduced recently,^{13d,e} we have considered the possibility to design chain compounds where the Ln centers are linked to ferromagnetic spin-clusters. Such a situation has been shown to reinforce the exchange interactions between the Ln and the coordinated spins and allowed for obtaining true molecular magnets.¹⁴ The huge library of metal-NIT complexes provided a candidate to probe the idea, namely the [Cu(NIT-3Py)]₂ ring system (NIT-3Py stands for 2-(3-pyridyl)-4,4,5,5-tetramethylimidazoline-1-oxyl-3-oxide radical) described by Rey et al.¹⁵ Herein we employed NIT-3Py (Chart 1), Cu(II), and Ln(III) reagents in a one-pot reaction to form unprecedented 1D 2p-3d-4f coordination polymers, namely, {[Ln(hfac)₃][Cu(hfac)₂(NIT-3Py)]₂·C₆H₁₄}_n (Ln = Y, 1; Gd, 2; Tb, 3; Dy, 4; hfac = hexafluoroacetylacetonate), in which cyclic [Cu(NIT-3py)]₂ units are bridged by Ln centers. Ferromagnetic interactions were observed in all four compounds, and the Tb derivative showed frequency-dependent out-of-phase signals indicative of slow relaxation of its magnetization.

Received: August 3, 2015

Published: September 24, 2015

Chart 1. Coordination Mode of the Radical Ligand NIT-3Py in Complexes 1–4



EXPERIMENTAL SECTION

Materials and Methods. All the reagents were commercially purchased and used as received. The preparation of the radical ligand NIT-3py was followed a reported procedure.¹⁶ Elemental analyses for carbon, hydrogen, and nitrogen were carried out with a Perkin–Elmer 240 elemental analyzer. Infrared spectra were recorded in KBr pellets on a Bruker Tensor 27 Spectrophotometer in the 400–4000 cm^{-1} region. Magnetic measurements were performed on Quantum Design SQUID VSM/MPMS-5 magnetometers using crystalline powder samples mixed with the grease. AC susceptibilities data for **3** were recorded on a Quantum Design PPMS-9. The magnetic susceptibility data were corrected for the diamagnetic contribution of the sample holders and for all the atoms using Pascal's tables.¹⁷

Preparation of $\{[\text{Ln}(\text{hfac})_3][\text{Cu}(\text{hfac})_2(\text{NIT-3Py})]_2 \cdot \text{C}_6\text{H}_{14}\}_n$ [$\text{Ln} = \text{Y}$ (1**), Gd (**2**), Tb (**3**), Dy (**4**)].** Solid $\text{Ln}(\text{hfac})_3 \cdot 2\text{H}_2\text{O}$ (0.02 mmol) and $\text{Cu}(\text{hfac})_2 \cdot 2\text{H}_2\text{O}$ (0.017 g, 0.04 mmol) were dissolved in *n*-hexane (15 mL) and heated to reflux for 2 h. Then a solution of NIT-3py (0.01 g, 0.04 mmol) in dry CH_2Cl_2 (5 mL) was added dropwise to the hot solution. The resulting mixture was stirred for 30 min and filtered ones cooled to ambient temperature. The filtrate was kept undisturbed for slow evaporation. After 2 days, the rectangular blue crystals of X-ray quality were collected by filtration. Yield: 42% for **1**, 32% for **2**, 46% for **3**, and 48% for **4**. Anal. Calcd for $\text{C}_{59}\text{H}_{39}\text{Cu}_2\text{F}_{42}\text{N}_6\text{O}_{18}\text{Y}$ (**1** without solvent molecule): C, 33.21; H, 1.84; N, 3.94. Found: C, 33.86; H, 2.16; N, 3.89. IR(**1**): 3137(m), 2359(m), 1655(s), 1493(s), 1262(s), 1210(s), 1148(s), 805(m), 668(m), 589(m). Anal. Calcd for $\text{C}_{59}\text{H}_{39}\text{Cu}_2\text{F}_{42}\text{N}_6\text{O}_{18}\text{Gd}$ (**2** without solvent molecule): C, 32.18; H, 1.79; N, 3.82. Found: C, 32.78; H, 2.14; N, 3.87. IR (**2**): 3139(m), 2358(m), 1654(s), 1495(s), 1261(s), 1210(s), 1147(s), 806(m), 667(m), 587(m). Anal. Calcd for $\text{C}_{59}\text{H}_{39}\text{Cu}_2\text{F}_{42}\text{N}_6\text{O}_{18}\text{Tb}$ (**3** without solvent molecule): C, 32.15; H, 1.78; N, 3.81. Found: C, 32.67; H, 2.12; N, 3.85. IR (**3**): 3138(m), 2361(m), 1654(s), 1498(s), 1262(s), 1211(s), 1146(s), 806(m), 668(m), 589(m). Anal. Calcd for $\text{C}_{59}\text{H}_{39}\text{Cu}_2\text{F}_{42}\text{N}_6\text{O}_{18}\text{Dy}$ (**4** without solvent molecule): C, 32.10; H, 1.78; N, 3.81. Found: C, 32.65; H, 2.15; N, 3.88. IR (**4**): 3138(m), 2361(m), 1654(s), 1498(s), 1262(s), 1211(s), 1146(s), 806(m), 668(m), 589(m).

X-ray Crystallography. Single-crystal structure investigations were performed on a Rigaku Saturn diffractometer equipped with a CCD area detector and graphite-monochromated Mo/ $K\alpha$ radiation ($\lambda = 0.71073 \text{ \AA}$) at 113 K. Empirical absorption corrections based on symmetry equivalent reflections were applied. The structure solution was done with direct methods using SHELXS-97, and structure refinements were performed against $|F|^2$ by a full-matrix least-squares procedure using SHELXL-97.¹⁸ Anisotropic thermal parameters were assigned to all non-hydrogen atoms. Hydrogen atoms were placed in calculated, ideal positions and were refined isotropically as riding on their respective C atoms. The restraint command “isor” and “ealp” was employed to restrain the fluorine atoms so as to avoid the ADP problems on them. For **1**, the inherent poor quality of the crystals resulted in weak diffraction and a slightly high R_{int} value, thus leading to a relatively high R value. However, it did not affect the determination of the crystal structure, and the bond lengths and angles for **1** are consistent with that of **2–4**. A detailed summary of the crystallographic and structure refinement data of **1–4** is given in Table S1 in the Supporting Information.

RESULTS AND DISCUSSION

The compounds $\{[\text{Ln}(\text{hfac})_3][\text{Cu}(\text{hfac})_2(\text{NIT-3Py})]_2 \cdot \text{C}_6\text{H}_{14}\}_n$ ($\text{Ln} = \text{Y}$, **1**; Gd , **2**; Tb , **3**; Dy , **4**; hfac = hexafluoroacetylacetonate) were obtained as crystalline materials from the reaction mixtures containing the NIT-3Py ligand and the activated $\text{Ln}(\text{hfac})_3$ and $\text{Cu}(\text{hfac})_2$ complexes. The highly selective association pattern resulting from such an one-pot reaction can be ascribed to the strong coordination affinity of the pyridine unit for Cu(II) which drives the formation of the $[\text{CuNIT-3Py}]_2$ unit. The latter then acts as a metallo-ligand toward the Ln ions by means of its available aminoxy groups.

Description of the Structures. The crystal structures of **1–4** revealed that the four compounds are isomorphous. Therefore, only the structure of **3** is described as the representative.

Complex **3** crystallizes in the monoclinic space group $P2_1/c$ and consists of a 1D coordination polymer assembled from cyclic $[\text{CuNIT}]_2$ moieties and $\text{Gd}(\text{hfac})_3$ units (Figure 1). The

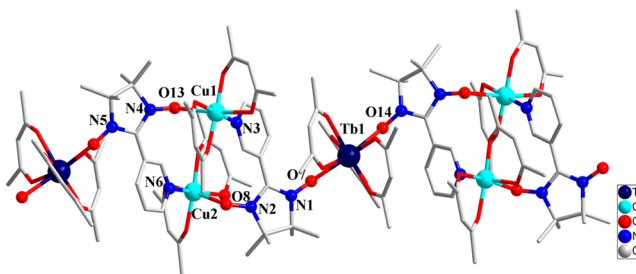


Figure 1. Molecular structure for **3** (all hydrogen and fluorine atoms are omitted for clarity).

asymmetric unit incorporates two independent $\text{Cu}(\text{hfac})_2$ moieties, one $\text{Tb}(\text{hfac})_3$, two NIT-3Py radical ligands, and one solvent molecule (C_6H_{14}). Each NIT-3Py is linked to two Cu ions by means of one NO group and the pyridine nitrogen atom, thus yielding the centro-symmetric cyclic $[\text{Cu}(\text{hfac})_2\text{NIT-3Py}]_2$ dimer. Each cyclic dimer behaves as bidentate ligand via its two NO groups connecting two $\text{Tb}(\text{hfac})_3$ units, and each Ln center interacts with two $[\text{Cu}(\text{hfac})_2\text{NIT-3Py}]_2$, thus developing a 1D organization along the *c* axis. Each Cu(II) is six-coordinated with one oxygen and one nitrogen atom from two NIT-3Py and four oxygen atoms from two chelating hfac ligands. For **3**, the equatorial $\text{Cu}-\text{O}(\text{hfac})/\text{N}$ distances are in the range of 1.938(3)–2.030(4) \AA (a selection of bond distances and angles are listed in Table 1). The axial positions are occupied by two oxygen atoms from a NO and one hfac group, respectively. The $\text{Cu}-\text{O}(\text{rad})$ bond distances ($\text{Cu}(1)-\text{O}(13)$ and $\text{Cu}(2)-\text{O}(8)$) are significantly longer than the basal bond lengths because of the Jahn–Teller effect.^{15,19} The related $\text{Cu}-\text{O}-\text{N}$ angles are 125.1(2)° and 117.4(3)°. The Tb(III) ion is eight-coordinated with six oxygen atoms from three hfac ligands and two oxygen atoms from two nitroxide groups of the radicals. The shapes of the coordination sphere around the Tb as well as for the other Ln derivatives were analyzed using SHAPE software,²⁰ revealing a distorted triangular dodecahedron geometry (D_{2d} ; Table S2 in Supporting Information). The $\text{Tb}-\text{O}(\text{radical})$ distances ($\text{Tb}-\text{O}(7/14)$) and the $\text{Tb}-\text{O}(\text{hfac})$ bond lengths are similar to those observed previously in $\text{Ln}(\text{hfac})_3$ -nitronyl nitroxide radical complexes.^{10,21} The $\text{O}(\text{rad})-\text{Tb}-\text{O}(\text{rad})$ angle is 136.4(1)°. In the chain, the $\text{Cu}-\text{Cu}$ separation in the dimer unit is 5.917 \AA , and the distances between Tb^{III} and two

Table 1. Selected Bond Lengths (Å) and Angles (deg) for Complexes 1–4^a

1		2		3		4	
Y(1)–O(1)	2.363(5)	Gd(1)–O(2)	2.381(3)	Tb(1)–O(1)	2.353(3)	Dy(1)–O(2)	2.359(3)
Y(1)–O(2)	2.295(6)	Gd(1)–O(3)	2.358(3)	Tb(1)–O(2)	2.338(5)	Dy(1)–O(3)	2.365(3)
Y(1)–O(3)	2.367(5)	Gd(1)–O(4)	2.389(3)	Tb(1)–O(3)	2.337(3)	Dy(1)–O(4)	2.327(3)
Y(1)–O(4)	2.314(5)	Gd(1)–O(5)	2.356(3)	Tb(1)–O(4)	2.382(3)	Dy(1)–O(5)	2.345(3)
Y(1)–O(5)	2.306(5)	Gd(1)–O(6)	2.375(3)	Tb(1)–O(5)	2.326(3)	Dy(1)–O(6)	2.329(3)
Y(1)–O(6)	2.344(5)	Gd(1)–O(7)	2.392(3)	Tb(1)–O(6)	2.378(3)	Dy(1)–O(7)	2.305(3)
Y(1)–O(7)	2.349(6)	Gd(1)–O(8)	2.334(3)	Tb(1)–O(7)	2.346(3)	Dy(1)–O(8)	2.364(3)
Y(1)–O(14)#1	2.321(6)	Gd(1)–O(9)#1	2.356(3)	Tb(1)–O(14)#1	2.376(3)	Dy(1)–O(9)	2.331(3)
Cu(1)–O(10)	1.957(6)	Cu(1)–O(11)	1.953(3)	Cu(1)–O(12)	1.952(3)	Cu(1)–O(15)	1.935(3)
Cu(1)–O(12)	1.966(6)	Cu(1)–O(14)	1.961(3)	Cu(1)–O(9)	1.938(3)	Cu(1)–O(18)	1.947(3)
Cu(1)–O(11)	1.983(5)	Cu(1)–O(13)	1.982(3)	Cu(1)–O(11)	1.989(3)	Cu(1)–O(17)	1.985(3)
Cu(1)–N(3)	2.010(6)	Cu(1)–N(4)#2	2.009(4)	Cu(1)–N(3)	2.030(4)	Cu(1)–N(6)#1	2.026(4)
Cu(1)–O(9)	2.228(6)	Cu(1)–O(12)	2.227(3)	Cu(1)–O(10)	2.282(3)	Cu(1)–O(16)	2.273(3)
Cu(1)–O(13)	2.508(5)	Cu(1)–O(10)	2.509(3)	Cu(1)–O(13)	2.486(3)	Cu(1)–O(1)	2.483(3)
Cu(2)–O(16)	1.931(6)	Cu(2)–O(18)	1.929(3)	Cu(2)–O(18)	1.961(3)	Cu(2)–O(14)	1.957(3)
Cu(2)–O(17)	1.942(7)	Cu(2)–O(15)	1.951(3)	Cu(2)–O(15)	1.969(3)	Cu(2)–O(11)	1.958(3)
Cu(2)–O(18)	2.002(5)	Cu(2)–O(16)	1.983(3)	Cu(2)–O(16)	1.984(3)	Cu(2)–O(12)	1.985(3)
Cu(2)–N(6)	2.028(6)	Cu(2)–N(1)	2.023(4)	Cu(2)–N(6)	2.009(4)	Cu(2)–N(3)#2	2.000(4)
Cu(2)–O(15)	2.282(6)	Cu(2)–O(17)	2.281(3)	Cu(2)–O(17)	2.225(3)	Cu(2)–O(13)	2.220(3)
Cu(2)–O(8)	2.488(5)	Cu(2)–O(1)#2	2.508(3)	Cu(2)–O(8)	2.508(3)	Cu(2)–O(10)	2.506(3)
O(2)–Y(1)–O(7)	89.9(2)	O(8)–Gd(1)–O(2)	89.7(1)	O(5)–Tb(1)–O(7)	99.6(1)	O(7)–Dy(1)–O(2)	89.3(1)
O(5)–Y(1)–O(7)	106.4(2)	O(5)–Gd(1)–O(2)	106.7(1)	O(3)–Tb(1)–O(7)	76.2(1)	O(4)–Dy(1)–O(2)	75.4(1)
O(4)–Y(1)–O(7)	74.6(2)	O(9)#1–Gd(1)–O(2)	136.6(1)	O(7)–Tb(1)–O(2)	95.8(1)	O(6)–Dy(1)–O(2)	106.6(1)
O(14)#1–Y(1)–O(7)	136.7(2)	O(3)–Gd(1)–O(2)	75.3(1)	O(7)–Tb(1)–O(1)	150.1(1)	O(9)–Dy(1)–O(2)	136.5(1)
O(6)–Y(1)–O(7)	73.5(2)	O(6)–Gd(1)–O(2)	73.2(1)	O(7)–Tb(1)–O(14) #1	136.4(1)	O(5)–Dy(1)–O(2)	73.3(1)
O(7)–Y(1)–O(1)	150.4(2)	O(2)–Gd(1)–O(4)	70.4(1)	O(7)–Tb(1)–O(6)	71.6(1)	O(2)–Dy(1)–O(3)	70.6(1)
N(1)–O(7)–Y(1)	139.9(5)	O(2)–Gd(1)–O(7)	150.2(1)	O(7)–Tb(1)–O(4)	70.1(1)	O(2)–Dy(1)–O(8)	150.0(1)
O(7)–Y(1)–O(3)	70.9(2)	N(6)–O(2)–Gd(1)	139.7(3)	N(1)–O(7)–Tb(1)	141.2(3)	N(4)–O(9)–Dy(1)	141.0(3)
O(10)–Cu(1)–O(13)	87.2(2)	O(11)–Cu(1)–O(10)	87.5(1)	O(9)–Cu(1)–O(13)	89.3(1)	O(15)–Cu(1)–O(1)	89.3(1)
O(12)–Cu(1)–O(13)	100.0(2)	O(14)–Cu(1)–O(10)	100.2(1)	O(12)–Cu(1)–O(13)	90.1(1)	O(18)–Cu(1)–O(1)	90.0(1)
O(11)–Cu(1)–O(13)	87.3(2)	O(13)–Cu(1)–O(10)	86.8(1)	O(11)–Cu(1)–O(13)	90.0(1)	O(17)–Cu(1)–O(1)	89.8(1)
N(3)–Cu(1)–O(13)	79.1(2)	N(4)#2–Cu(1)– O(10)	79.4(1)	N(3)–Cu(1)–O(13)	172.6(1)	O(16)–Cu(1)–O(1)	172.5(1)
O(9)–Cu(1)–O(13)	173.9(2)	O(12)–Cu(1)–O(10)	173.7(1)	O(10)–Cu(1)–O(13)	172.6(1)	N(6)#1–Cu(1)–O(1)	88.2(1)
N(4)–O(13)–Cu(1)	117.4(4)	N(2)–O(10)–Cu(1)	117.0(3)	N(4)–O(13)–Cu(1)	125.1(2)	N(1)–O(1)–Cu(1)	125.3(3)

^aSymmetry transformations used to generate equivalent atoms: #1: $x, -y + 1/2, z + 1/2$ for 1; #1: $x + 1, y, z$; #2: $x - 1, -y + 1/2, z - 1/2$ for 2; #1: $x, -y + 1/2, z + 1/2$ for 3; #1: $x, -y + 1/2, z - 1/2$; #2: $x, -y + 1/2, z + 1/2$ for 4.

Cu^{II} ions bridged by a NIT are 7.929 and 8.311 Å. The crystal packing diagram of **3** is shown in Figure S6 in the Supporting Information. The shortest interchain metal–metal separation is found between two Cu^{II} with 9.312 Å, while the shortest Tb–Cu and Tb–Tb distances are 10.975 and 11.710 Å, respectively. Such large separations between magnetic centers (especially, Ln ions) of neighboring chains reduce the possible dipolar interactions between the metals.^{9c,10a,b,h} Thus, the interchain magnetic interactions can be anticipated to be very weak in these compounds, which is indeed confirmed by the $\chi_M T$ behaviors for **2**–**4** that steadily increase down to 2 K (vide infra).

Magnetic Properties. The temperature dependences of the magnetic susceptibility for **1**–**4** were recorded under a 1 kOe DC field from 300 to 2 K; results are shown in Figure 2 as $\chi_M T$ versus T plots where χ_M corresponds to the susceptibility for a formula unit without solvent molecules.

For **1** and **2**, the room temperature $\chi_M T$ value is 1.75 cm³ mol⁻¹ K and 10.51 cm³ mol⁻¹ K, respectively, in good agreement with the expected values of 1.6 and 9.53 cm³ mol⁻¹ K, respectively, for **1** and **2**, considering one paramagnetic Ln^{III} ion (Y^{III}, diamagnetic; Gd^{III}, ⁸S_{7/2}; $S = 7/2$; $L = 0$; $g = 2$) plus

two isolated Cu^{II} ions ($S = 1/2$, $g = 2.2$) and two radicals ($S = 1/2$, $g = 2.0$). For **1**, the value for $\chi_M T$ increases slowly from 300 to 34 K to reach a maximum of 2.09 cm³ K mol⁻¹ and then sharply decreases to a value of 0.62 cm³ K mol⁻¹ at 2 K, while for **2**, $\chi_M T$ continually increases to reach 23.11 cm³ K mol⁻¹ at 2 K. These behaviors confirm the ferromagnetic contributions anticipated for the Cu–NIT and Gd–NIT exchange interactions and the absence of sizable interchain interactions. For **1**, three exchange pathways may contribute to the observed behavior: (i) the direct radical–Cu exchange mediated by the NO–Cu bond (J_1), (ii) the Cu–radical interaction through the pyridine ring (J_2), and (iii) the next-neighbor radical–radical interaction through Y^{III} ion (J_3). MAGPACK was used to simulate the magnetic susceptibilities based on a closed ring model²² comprising three [Y–{Cu₂NIT₂}] cluster units with the J_1 , J_2 , and J_3 exchange interactions (Scheme 1). The Hamiltonian describing this situation is given by

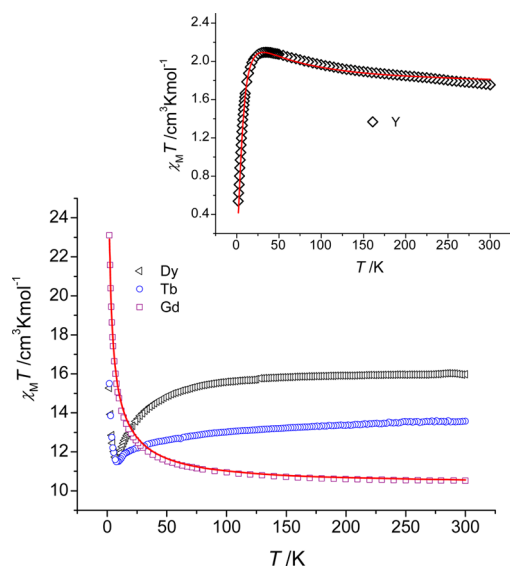
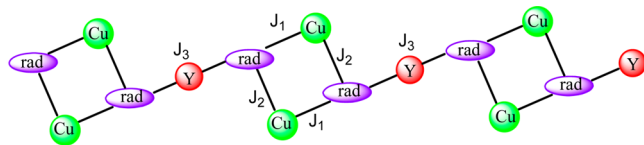


Figure 2. $\chi_M T$ versus T plots for complexes 1–4. The red solid lines represent the calculated behavior for 1 and 2 (see text).

$$\hat{H} = -2J_1 \sum_{i=1}^6 \hat{S}_{\text{Rad}_i} \hat{S}_{\text{Cu}_i} - 2J_2 \sum_{i=0}^2 (\hat{S}_{\text{Rad}_{2i+1}} \hat{S}_{\text{Cu}_{2i+2}} + \hat{S}_{\text{Rad}_{2i+2}} \hat{S}_{\text{Cu}_{2i+1}}) - 2J_3 (\hat{S}_{\text{Rad}_2} \hat{S}_{\text{Rad}_3} + \hat{S}_{\text{Rad}_4} \hat{S}_{\text{Rad}_5} + \hat{S}_{\text{Rad}_6} \hat{S}_{\text{Rad}_1})$$

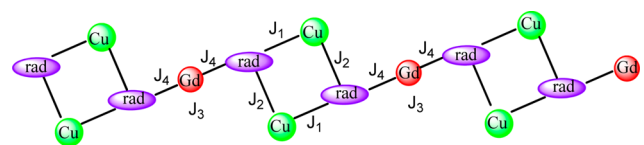
Scheme 1. Magnetic Exchange Pathways in 1



The best agreement between calculated and experimental behaviors was obtained for $J_1 = 18.96 \text{ cm}^{-1}$, $J_2 = 3.75 \text{ cm}^{-1}$, $J_3 = -7.56 \text{ cm}^{-1}$, and $g = 2.15$ (Figure 2). The obtained exchange parameters are consistent in those reported for related copper(II)/Y–nitronyl nitroxide.²³ The ferromagnetic Cu^{II} and NIT interaction via pyridine group (J_2) is rationalized by a spin-polarization mechanism (Scheme S1 in the SI).

For 2, in addition to the above-mentioned exchange interactions (J_1 , J_2 , J_3), the operative exchange interactions comprise the Gd-rad interaction (J_4 ; Scheme 2). Considering two cluster units (the Hamiltonian describing the spin system is given in eq 1), MAGPACK allowed fitting of the magnetic susceptibilities, yielding $J_1 = 18.85 \text{ cm}^{-1}$, $J_2 = 3.46 \text{ cm}^{-1}$, $J_3 = -7.25 \text{ cm}^{-1}$, $J_4 = 1.85 \text{ cm}^{-1}$, and $g = 2.10$. The value found for J_4 is in agreement with a weak ferromagnetic interaction

Scheme 2. Magnetic Exchange Pathways in Complex 2



between Gd(III) and the aminoxyl moiety as usually found for Gd-NIT complexes.^{21b–d,24}

$$\hat{H} = -2J_1 (\hat{S}_{\text{Rad}_1} \hat{S}_{\text{Cu}_1} + \hat{S}_{\text{Rad}_2} \hat{S}_{\text{Cu}_2} + \hat{S}_{\text{Rad}_3} \hat{S}_{\text{Cu}_3} + \hat{S}_{\text{Rad}_4} \hat{S}_{\text{Cu}_4}) - 2J_2 (\hat{S}_{\text{Rad}_1} \hat{S}_{\text{Cu}_2} + \hat{S}_{\text{Rad}_2} \hat{S}_{\text{Cu}_1} + \hat{S}_{\text{Rad}_3} \hat{S}_{\text{Cu}_4} + \hat{S}_{\text{Rad}_4} \hat{S}_{\text{Cu}_3}) - 2J_4 (\hat{S}_{\text{Rad}_2} \hat{S}_{\text{Gd}_1} + \hat{S}_{\text{Rad}_3} \hat{S}_{\text{Gd}_1} + \hat{S}_{\text{Rad}_4} \hat{S}_{\text{Gd}_2} + \hat{S}_{\text{Rad}_1} \hat{S}_{\text{Gd}_2}) - 2J_3 (\hat{S}_{\text{Rad}_2} \hat{S}_{\text{Rad}_3} + \hat{S}_{\text{Rad}_4} \hat{S}_{\text{Rad}_1}) \quad (1)$$

The field dependence of magnetization for 2 exhibits a fast increase for low fields and reaches $11.5 \text{ N}\beta$ at 7T, in agreement with the expected saturation values of $11 \text{ N}\beta$. As shown in Figure 3, over the entire field range, the experimental

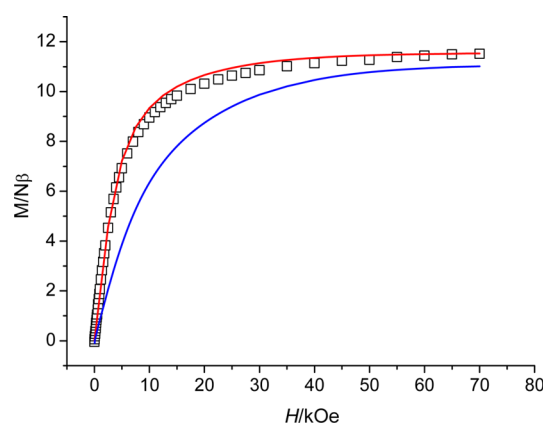


Figure 3. M versus H curves for complex 2. The solid lines represent calculated behavior (red lines, calculated with the best fit parameters deduced from $\chi_M T$ versus T ; blue lines, calculated with Brillouin function).

magnetization of 2 is higher than the magnetization calculated with the Brillouin function for noncoupled one $S = 7/2$ and four $S = 1/2$ spin centers, confirming the overall ferromagnetic interactions in complex 2. Furthermore, the experimental behavior is perfectly reproduced by the M vs H behavior calculated with the exchange parameters deduced from the modeling of $\chi_M T$ versus T .

For 3 and 4, the $\chi_M T$ values at room temperature are $13.60 \text{ cm}^3 \text{ K mol}^{-1}$ (3) and $15.95 \text{ cm}^3 \text{ K mol}^{-1}$ (4), in agreement with the anticipated value of respectively 13.46 and $15.82 \text{ cm}^3 \text{ K mol}^{-1}$, considering one isolated Ln^{III} ion (Tb^{III} : ${}^7\text{F}_6$, $S = 3$, $L = 3$, $g = 3/2$; Dy^{III} : ${}^6\text{H}_{15/2}$, $S = 5/2$, $L = 5$, $g = 4/3$) plus two isolated Cu^{II} ions ($S = 1/2$, $g = 2.2$) and two radicals ($S = 1/2$, $g = 2.0$). Upon cooling, the $\chi_M T$ values of 3 and 4 decrease slowly to $11.5 \text{ cm}^3 \text{ K mol}^{-1}$ and $11.7 \text{ cm}^3 \text{ K mol}^{-1}$, respectively, at 8 K and then steeply increase to $15.5 \text{ cm}^3 \text{ K mol}^{-1}$ and $15.3 \text{ cm}^3 \text{ K mol}^{-1}$, respectively, at 2 K. The increase of $\chi_M T$ at low temperatures is in agreement with the anticipated ferromagnetic interaction between the Ln ions and the coordinated organic radical,²⁵ while the initial decrease seen for higher T is the result of crystal field effects.^{25,26} The field dependent magnetizations for 3 and 4 measured at 2 K exhibit a fast rise for low fields followed by a more gradual but continuous increases to $6.7 \text{ N}\beta$ and $6.9 \text{ N}\beta$, respectively, at 5T (Figures S8 and S9 in the Supporting Information). The saturation is not reached, which can be attributed to the magnetic anisotropy of the Ln ions in 3 and 4.²⁷

AC magnetic susceptibility measurements were performed for 3 and 4 to probe dynamic magnetic behaviors. Under zero

dc fields, frequency dependence of the in- (χ_M') and out-of-phase (χ_M'') signal is observed for **3**, revealing slow relaxation of its magnetization (Figure 4). However, no peak maxima are

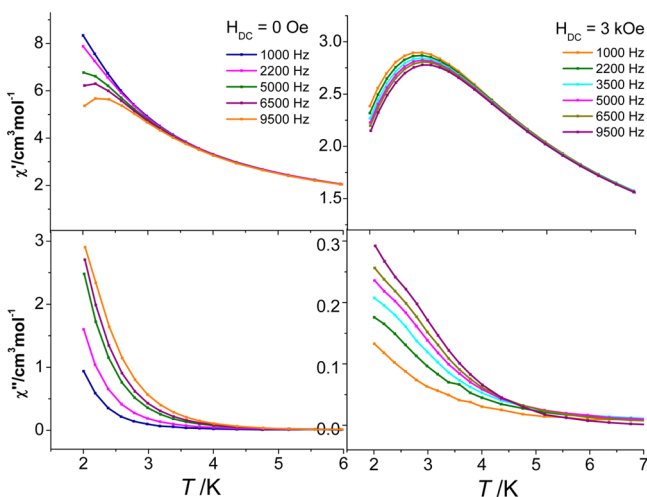


Figure 4. Temperature dependence of the in-phase and out-of-phase components of ac susceptibility for **3** in zero dc field (left) and in a 3 kOe dc field (right).

observed for χ_M'' above 2 K. A static magnetic field was applied to suppress any possible quantum tunneling process (QTM). With a 3 kOe DC field, the in-phase susceptibility curves show frequency dependent peaks, yet while clear curvature changes become apparent for the χ_M'' components, no peak maxima are observed. For complex **4**, the χ_M'' signal does not deviate from zero either with or without an applied static field (Figure S10 in the Supporting Information).

CONCLUDING REMARKS

These 2p-3d-4f chain compounds illustrate the design potential of the hetero-tri-spin approach. Playing with the coordination preferences of the radical-ligand, it becomes possible to obtain spin topologies more sophisticated than just alternating spin arrangements. Here, small ferromagnetic Cu-NIT aggregates have been generated in situ and subsequently involved as metallo-ligands for the Ln centers to yield 1D coordination polymers. The driving force for such a highly selective association scheme can be attributed to the robust coordination of the NIT-pyridine chelating to Cu. Related behavior can be anticipated for other 3d ions which may open interesting perspectives in the development of novel 2p-3d-4f magnetic systems. AC susceptibility confirms a slow relaxation processes for the Tb derivative; however the fast relaxations taking place at low T could not be canceled by an applied DC field. It is likely that these arise from weak interchain dipolar interactions.

This work demonstrates that functional nitronyl nitroxide radicals are an appealing way to construct novel 2p-3d-4f chain compounds with novel spin topologies and hopefully interesting magnetic properties.

ASSOCIATED CONTENT

Supporting Information

The Supporting Information is available free of charge on the ACS Publications website at DOI: 10.1021/acs.inorgchem.5b01761.

Crystal structure, packing diagram, chart for spin polarization mechanism, table for SHAPE analysis, and additional magnetic data (PDF)

X-ray crystallographic data in CIF format for complex **1** (CIF)

X-ray crystallographic data in CIF format for complex **2** (CIF)

X-ray crystallographic data in CIF format for complex **3** (CIF)

X-ray crystallographic data in CIF format for complex **4** (CIF)

AUTHOR INFORMATION

Corresponding Authors

*E-mail: llicun@nankai.edu.cn.

*E-mail: sutter@lcc-toulouse.fr.

Notes

The authors declare no competing financial interest.

ACKNOWLEDGMENTS

This work was supported by the National Natural Science Foundation of China (No. 21471083) and MOE Innovation Team (IRT13022) of China.

REFERENCES

- (1) (a) De Jongh, L. J.; Miedema, A. R. *Adv. Phys.* **1974**, *23*, 1–260. (b) Georges, R.; Borras-Almenar, J. J.; Coronado, E.; Curély, J.; Drillon, M. In *Magnetism: Molecules to Materials*; Müller, J. S., Drillon, M., Eds.; Wiley-VCH: Weinheim, 2002; Vol. 1, pp 1–47.
- (2) (a) Kobayashi, H. *Acta Crystallogr., Sect. B: Struct. Crystallogr. Cryst. Chem.* **1978**, *34*, 2818–2825. (b) Bray, J. W.; Hart, H. R., Jr.; Interrante, L. V.; Jacobs, I. S.; Kasper, J. S.; Watkins, G. D.; Wee, S. H.; Bonner, J. C. *Phys. Rev. Lett.* **1975**, *35*, 744–747. (c) Takaishi, S.; Tobu, Y.; Kitagawa, H.; Goto, A.; Shimizu, T.; Okubo, T.; Mitani, T.; Ikeda, R. *J. Am. Chem. Soc.* **2004**, *126*, 1614–1615. (d) Mitsumi, M.; Yoshida, Y.; Kohyama, A.; Kitagawa, Y.; Ozawa, Y.; Kobayashi, M.; Toriumi, K.; Tadokoro, M.; Ikeda, N.; Okumura, M.; Kurmoo, M. *Inorg. Chem.* **2009**, *48*, 6680–6691.
- (3) (a) Haldane, F. D. M. *Phys. Rev. Lett.* **1983**, *50*, 1153–1156. (b) Granroth, G. E.; Meisel, M. W.; Chaparala, M.; Jolicoeur, Th.; Ward, B. H.; Talham, D. R. *Phys. Rev. Lett.* **1996**, *77*, 1616–1619. (c) Darriet, J.; Regnault, L. P. *Solid State Commun.* **1993**, *86*, 409–412. (d) Jotzu, G.; Messer, M.; Desbuquois, R.; Lebrat, M.; Uehlinger, T.; Greif, D.; Esslinger, T. *Nature* **2014**, *515*, 237–240. (e) Hase, M.; Soda, M.; Masuda, T.; Kawana, D.; Yokoo, T.; Itoh, S.; Matsuo, A.; Kindo, K.; Kohno, M. *Phys. Rev. B: Condens. Matter Mater. Phys.* **2014**, *90*, 024416.
- (4) Glauber, R. J. *J. Math. Phys.* **1963**, *4*, 294–307.
- (5) (a) Caneschi, A.; Gatteschi, D.; Lalioi, N.; Sangregorio, C.; Sessoli, R.; Venturi, G.; Vindigni, A.; Rettori, A.; Pini, M. G.; Novak, M. A. *Angew. Chem., Int. Ed.* **2001**, *40*, 1760–1763. (b) Clérac, R.; Miyasaka, H.; Yamashita, M.; Coulon, C. *J. Am. Chem. Soc.* **2002**, *124*, 12837–12844. (c) Miyasaka, H.; Madanbashi, T.; Sugimoto, K.; Nakazawa, Y.; Wernsdorfer, W.; Sugiura, K.-I.; Yamashita, M.; Coulon, C.; Clérac, R. *Chem. - Eur. J.* **2006**, *12*, 7028–7040. (d) Ishikawa, R.; Katoh, K.; Breedlove, B. K.; Yamashita, M. *Inorg. Chem.* **2012**, *51*, 9123–9131.
- (6) (a) Wang, S.; Zuo, J.-L.; Gao, S.; Song, Y.; Zhou, H.-C.; Zhang, Y.-Z.; You, X.-Z. *J. Am. Chem. Soc.* **2004**, *126*, 8900–8901. (b) Sun, H. L.; Wang, Z. M.; Gao, S. *Chem. - Eur. J.* **2009**, *15*, 1757–1764. (c) Chen, Q.; Meng, Y.-S.; Zhang, Y.-Q.; Jiang, S.-D.; Sun, H.-L.; Gao, S. *Chem. Commun.* **2014**, *50*, 10434–10437. (d) Jia, L.; Chen, Q.; Meng, Y.-S.; Sun, H.-L.; Gao, S. *Chem. Commun.* **2014**, *50*, 6052–6055.
- (7) (a) Caneschi, A.; Gatteschi, D.; Sessoli, R.; Rey, P. *Acc. Chem. Res.* **1989**, *22*, 392–398. (b) Bogani, L. *J. Appl. Phys.* **2011**, *109*, 07B115.

- (8) Caneschi, A.; Gatteschi, D.; Rey, P. *Prog. Inorg. Chem.* **1991**, *39*, 331–421.
- (9) (a) Ishii, N.; Okamura, Y.; Chiba, S.; Nogami, T.; Ishida, T. *J. Am. Chem. Soc.* **2008**, *130*, 24–25. (b) Ishida, T.; Okamura, Y.; Watanabe, I. *Inorg. Chem.* **2009**, *48*, 7012–7014. (c) Vaz, M. G. F.; Cassaro, R. A. A.; Akpınar, H.; Schlueter, J. A.; Lahti, P. M.; Novak, M. A. *Chem. - Eur. J.* **2014**, *20*, 5460–5467.
- (10) (a) Bogani, L.; Sangregorio, C.; Sessoli, R.; Gatteschi, D. *Angew. Chem., Int. Ed.* **2005**, *44*, 5817–5821. (b) Bernot, K.; Bogani, L.; Caneschi, A.; Gatteschi, D.; Sessoli, R. *J. Am. Chem. Soc.* **2006**, *128*, 7947–7956. (c) Bernot, K.; Bogani, L.; Sessoli, R.; Gatteschi, D. *Inorg. Chim. Acta* **2007**, *360*, 3807–3812. (d) Liu, R.-N.; Li, L.-C.; Wang, X.-L.; Yang, P.-P.; Wang, C.; Liao, D.-Z.; Sutter, J.-P. *Chem. Commun.* **2010**, *46*, 2566–2568. (e) Liu, R.-N.; Ma, Y.; Yang, P.-P.; Song, X.-Y.; Xu, G.-F.; Tang, J.-K.; Li, L.-C.; Liao, D.-Z.; Yan, S.-P. *Dalton Trans.* **2010**, *39*, 3321–3325. (f) Han, T.; Shi, W.; Niu, Z.; Na, B.; Cheng, P. *Chem. - Eur. J.* **2013**, *19*, 994–1001. (g) Hu, P.; Wang, X.-F.; Ma, Y.; Wang, Q.-L.; Li, L.-C.; Liao, D.-Z. *Dalton Trans.* **2014**, *43*, 2234–2243. (h) Wang, X.-F.; Li, Y.-G.; Hu, P.; Wang, J.-J.; Li, L.-C. *Dalton Trans.* **2015**, *44*, 4560–4567.
- (11) Bernot, K.; Luzon, J.; Sessoli, R.; Vindigni, A.; Thion, J.; Richeter, S.; Leclercq, D.; Larionova, J.; van der Lee, A. *J. Am. Chem. Soc.* **2008**, *130*, 1619–1627.
- (12) Bartolome, F.; Bartolome, J.; Benelli, C.; Caneschi, A.; Gatteschi, D.; Paulsen, C.; Pini, M. G.; Rettori, A.; Sessoli, R.; Volokitin, Y. *Phys. Rev. Lett.* **1996**, *77*, 382–385.
- (13) (a) Madalan, A. M.; Roesky; Andruh, M.; Noltemeyer, M.; Stanica, N. *Chem. Commun.* **2002**, 1638–1639. (b) Zhu, M.; Li, Y.-G.; Ma, Y.; Li, L.-C.; Liao, D.-Z. *Inorg. Chem.* **2013**, *52*, 12326–12328. (c) Escobar, L. B. L.; Guedes, G. P.; Soriano, S.; Speziali, N. L.; Jordão, A. K.; Cunha, A. C.; Ferreira, V. F.; Maxim, C.; Novak, M. A.; Andruh, M.; Vaz, M. G. F. *Inorg. Chem.* **2014**, *53*, 7508–7517. (d) Zhu, M.; Mei, X.-L.; Ma, Y.; Li, L.-C.; Liao, D.-Z.; Sutter, J.-P. *Chem. Commun.* **2014**, *50*, 1906–1908. (e) Zhu, M.; Hu, P.; Li, Y.-G.; Wang, X.-F.; Li, L.-C.; Liao, D.-Z.; Durga Prasad Goli, V. M. L.; Ramasesha, S.; Sutter, J.-P. *Chem. - Eur. J.* **2014**, *20*, 13356–13365. (f) Wang, Z.-X.; Zhang, X.; Zhang, Y.-Z.; Li, M.-X.; Zhao, H.; Andruh, M.; Dunbar, K. R. *Angew. Chem., Int. Ed.* **2014**, *53*, 11567–11570. (g) Wang, X.-F.; Hu, P.; Li, Y.-G.; Li, L.-C. *Chem. - Asian J.* **2015**, *10*, 325–328. (h) Wang, C.; Lin, S.-Y.; Shi, W.; Cheng, P.; Tang, J.-K. *Dalton Trans.* **2015**, *44*, 5364–5368.
- (14) Dhers, S.; Costes, J.-P.; Guionneau, P.; Paulsen, C.; Vendier, L.; Sutter, J.-P. *Chem. Commun.* **2015**, *51*, 7875–7878.
- (15) (a) Lanfranc de Panthou, F.; Belorizky, E.; Calemzuk, R.; Luneau, D.; Marcenat, C.; Ressouche, E.; Turek, P.; Rey, P. *J. Am. Chem. Soc.* **1995**, *117*, 11247–11253. (b) Lanfranc de Panthou, F.; Luneau, D.; Musin, R.; Öhrström, L.; Grand, A.; Turek, P.; Rey, P. *Inorg. Chem.* **1996**, *35*, 3484–3491.
- (16) Davis, M. S.; Morokuma, K.; Kreilick, R. W. *J. Am. Chem. Soc.* **1972**, *94*, 5588–5592.
- (17) Kahn, O. *Molecular Magnetism*; VCH: Weinheim, 1993.
- (18) (a) Sheldrick, G. M. *SHELXL-97*; University of Göttingen: Göttingen, Germany, 1997. (b) Sheldrick, G. M. *SHELXS-97*; University of Göttingen: Göttingen, Germany, 1997.
- (19) (a) Ishimaru, Y.; Kitano, M.; Kumada, H.; Koga, N.; Iwamura, H. *Inorg. Chem.* **1998**, *37*, 2273–2280. (b) Hirel, C.; Li, L.-C.; Brough, P.; Vostrikova, K.; Pécaut, J.; Mehdaoui, B.; Bernard, M.; Turek, P.; Rey, P. *Inorg. Chem.* **2007**, *46*, 7545–7552. (c) Gatteschi, D.; Laugier, J.; Rey, P.; Zanchini, C. *Inorg. Chem.* **1987**, *26*, 938–943.
- (20) (a) Casanova, D.; Llunell, M.; Alemany, P.; Alvarez, S. *Chem. - Eur. J.* **2005**, *11*, 1479–1494. (b) Llunell, M.; Casanova, D.; Cirera, J.; Alemany, P.; Alvarez, S. *SHAPE 2.1*; University of Barcelona: Barcelona, 2013.
- (21) (a) Benelli, C.; Caneschi, A.; Gatteschi, D.; Pardi, L.; Rey, P.; Shum, D. P.; Carlin, R. L. *Inorg. Chem.* **1989**, *28*, 272–275. (b) Benelli, C.; Caneschi, A.; Gatteschi, D.; Pardi, L.; Rey, P. *Inorg. Chem.* **1990**, *29*, 4223–4228. (c) Benelli, C.; Caneschi, A.; Gatteschi, D.; Pardi, L. *Inorg. Chem.* **1992**, *31*, 741–746. (d) Mei, X.-L.; Liu, R.-N.; Wang, C.; Yang, P.-P.; Li, L.-C.; Liao, D.-Z. *Dalton Trans.* **2012**, *41*, 2904–2909.
- (e) Coronado, E.; Gimenez-Saiz, C.; Recuenco, A.; Tarazon, A.; Romero, F.; Camon, A.; Luis, F. *Inorg. Chem.* **2011**, *50*, 7370–7372. (f) Hu, P.; Sun, Z.; Wang, X.-F.; Li, L.-C.; Liao, D.-Z.; Luneau, D. *New J. Chem.* **2014**, *38*, 4716–4721.
- (22) (a) Borrás-Almenar, J. J.; Clemente-Juan, J. M.; Coronado, E.; Tsukerblat, B. S. *Inorg. Chem.* **1999**, *38*, 6081–6088. (b) Borrás-Almenar, J. J.; Clemente-Juan, J. M.; Coronado, E.; Tsukerblat, B. S. *J. Comput. Chem.* **2001**, *22*, 985–991. (c) Borrás-Almenar, J. J.; Clemente-Juan, J. M.; Coronado, E.; Tsukerblat, B. S. *J. Inorg. Chem.* **1999**, *38*, 6081–6088.
- (23) (a) Caneschi, A.; Gatteschi, D.; Laugier, J.; Rey, P. *J. Am. Chem. Soc.* **1987**, *109*, 2191–2192. (b) Caneschi, A.; Gatteschi, D.; Grand, A.; Laugier, J.; Pardi, L.; Rey, P. *Inorg. Chem.* **1988**, *27*, 1031–1035. (c) Benelli, A.; Caneschi, D.; Gatteschi, L.; Pardi, P. *Inorg. Chem.* **1989**, *28*, 3230–3234. (d) Sutter, J.-P.; Kahn, M. L.; Golhen, S.; Ouahab, L.; Kahn, O. *Chem. - Eur. J.* **1998**, *4*, 571–576. (e) Wang, H. M.; Liu, Z. L.; Liu, C. M.; Zhang, D. Q.; Lu, Z. L.; Geng, H.; Shuai, Z. G.; Zhu, D. B. *Inorg. Chem.* **2004**, *43*, 4091–4098. (f) Liu, R.-N.; Li, L.-C.; Xing, X.-Y.; Liao, D.-Z. *Inorg. Chim. Acta* **2009**, *362*, 2253–2258. (g) Hu, P.; Zhang, C.-M.; Gao, Y.-Y.; Li, Y.-G.; Ma, Y.; Li, L.-C.; Liao, D.-Z. *Inorg. Chim. Acta* **2013**, *398*, 136–140.
- (24) (a) Lescop, C.; Luneau, D.; Rey, P.; Bussière, G.; Reber, C. *Inorg. Chem.* **2002**, *41*, 5566–5574. (b) Hu, P.; Zhu, M.; Mei, X.-L.; Tian, H.-X.; Ma, Y.; Li, L.-C.; Liao, D.-Z. *Dalton Trans.* **2012**, *41*, 14651–14656. (c) Wang, X. L. *Inorg. Chim. Acta* **2012**, *387*, 20–24. (d) Mei, X.-L.; Ma, Y.; Li, L.-C.; Liao, D.-Z. *Dalton Trans.* **2012**, *41*, 505–511.
- (25) (a) Kahn, M. L.; Sutter, J.-P.; Golhen, S.; Guionneau, P.; Ouahab, L.; Kahn, O.; Chasseau, D. *J. Am. Chem. Soc.* **2000**, *122*, 3413–3421. (b) Benelli, C.; Gatteschi, D. *Chem. Rev.* **2002**, *102*, 2369–2387.
- (26) (a) Sutter, J.-P.; Kahn, M. L.; Kahn, O. *Adv. Mater.* **1999**, *11*, 863–865. (b) Sutter, J.-P.; Kahn, M. L. In *Magnetism: Molecules to Materials*; Miller, J. S., Drillon, M., Eds.; Wiley-VCH: Weinheim, 2005; Vol. 5, pp 161–188.
- (27) (a) Lin, P. H.; Burchell, T. J.; Clérac, R.; Murugesu, M. *Angew. Chem., Int. Ed.* **2008**, *47*, 8848–8851. (b) Bernot, K.; Luzon, J.; Bogani, L.; Etienne, M.; Sangregorio, C.; Shanmugam, M.; Caneschi, A.; Sessoli, R.; Gatteschi, D. *J. Am. Chem. Soc.* **2009**, *131*, 5573–5579. (c) Xu, J.-X.; Ma, Y.; Liao, D.-Z.; Xu, G.-F.; Tang, J.-K.; Wang, C.; Zhou, N.; Yan, S.-P.; Cheng, P.; Li, L.-C. *Inorg. Chem.* **2009**, *48*, 8890–8896. (d) Zhang, P.; Zhang, L.; Wang, C.; Xue, S.; Lin, S.-Y.; Tang, J.-K. *J. Am. Chem. Soc.* **2014**, *136*, 4484–4487.